Charge and spin dynamics in VO2 nanorods

Kyu Won Lee, Hyocheon Kweon, Jitae Park, and Cheol Eui Lee

Citation: Appl. Phys. Lett. **94**, 233111 (2009); doi: 10.1063/1.3152780
View online: http://dx.doi.org/10.1063/1.3152780
View Table of Contents: http://apl.aip.org/resource/1/APPLAB/v94/i23
Published by the American Institute of Physics.

Charge and spin dynamics in VO_2 nanorods

Kyu Won Lee, Hyocheon Kweon, Jitae Park, and Cheol Eui Lee[a)]
Department of Physics and Institute for Nano Science, Korea University, Seoul 136-713, Republic of Korea

(Received 21 February 2009; accepted 19 May 2009; published online 10 June 2009)

Electrical conductivity and photoconductivity measurements were carried out on vanadium dioxide (VO_2) nanorods prepared by the hydrothermal treatment of vanadium pentoxide gels. While the structural properties of the nanorods resembled those of the Cr-doped VO_2, the charge and spin dynamics appears to resemble those of the Nb-doped VO_2. The magnetic and (photo)electrical properties of the nanorods can be understood in terms of localization of itinerant electrons giving rise to a spin-polarized ($S=3/2$) V^{4+} pair, dominant at higher temperatures, or to a ($S=1$) V^{3+} ion out of a V^{4+} ion pair, dominant at lower temperatures. © *2009 American Institute of Physics*. [DOI: 10.1063/1.3152780]

Vanadium dioxide (VO_2) has long been studied owing to the first-order metal-insulator transition at 340 K.[1–14] The electrical conductivity suddenly increases by several orders of magnitude through the low-temperature monoclinic (M_1) to the high-temperature rutile (R) structural phase transition. Meanwhile, $V_{1-x}Cr_xO_2$ bulk alloys[1–4] or bulk VO_2 with uniaxial stress applied[7] showed a new insulating (T or M_2) phase at low temperatures and, at intermediate compositions, successive $R \rightarrow M_2 \rightarrow T \rightarrow M_1$ structural phase transitions with decreasing temperature were observed.

In our recent work,[15] the structural and magnetic properties in vanadium dioxide (VO_2) nanorods prepared by the hydrothermal treatment of vanadium oxide xerogels were shown to be markedly different from the case of the bulk systems, a peculiar mixed phase of an insulating monoclinic structure (M_2) that is observed in the bulk systems under doping or stress and a high-temperature metallic rutile structure (R) being identified. Besides, a broad transition from a high-temperature magnetic phase to a low-temperature one, with quite distinct magnetic correlation strengths, was observed. In this work, we have carried out electrical conductivity and photoconductivity measurements in order to further elucidate the charge and spin dynamics of the VO_2 nanorods.

Vanadium dioxide nanorods with diameter of 60–300 nm and length of ~5 μm were synthesized by hydrothermal treatment of $V_2O_5 \cdot nH_2O$ gels obtained from dissolution of V_2O_5 in a solution of hydrogen peroxide, as described in our previous work.[15] For electrical measurements, polycrystalline powder was pressed at 2.29 MPa to obtain parallelepiped pellets. All the measurements were performed with decreasing temperature from 320 to 15 K by the standard two-probe method. Two gold wire electrodes with a 1 mm separation were put on the sample with conducting silver gelatin. The photocurrent measurements were made following illumination with light for about 30 s at each temperature with a Keithley 2400, using a 300 W xenon lamp as the white light source. The photocurrent was obtained as a function of time under 1 V forward bias by subtracting the current measured without illumination (dark current) from that measured with illumination.

a)Author to whom correspondence should be addressed. Electronic mail: rscel@korea.ac.kr.

In VO_2 single crystals, the first-order metal-insulator transition at 340 K is accompanied by a strong thermal hysteresis. The electrical conductance of VO_2 nanorods showed a weak and broad thermal hysteresis, which starts from 220 K and is not completed up to 400 K. Thus, the metal-insulator transition takes place in the nanorod pellet as well, the weak and broad thermal hystereses being attributed to size effects observed in nanosystems.[16,17]

Figure 1 shows the dark- and photoconductance plotted as $\ln(\sigma)$ versus $1/T$, displaying a small discontinuity at about 190 K. While the dark conductance below about 90 K was too small to be measured with precision, the photoconductance was nearly independent of temperature below about 80 K. In the semiconducting phase of VO_2 single crystals near the metal-insulator transition temperature, the electrical conductivity was found to follow the Arrhenius law with an activation energy of ~0.45 eV, which was attributed to the carrier concentration but not to the carrier mobility.[12] The electrical conductivity of VO_2 single crystals, deviating from the Arrhenius law with decreasing temperature, was suggested to follow a variable range hopping model.[13] In our previous work on VO_2 nanorods,[15] semiconducting (M_2) and metallic (R) phases were found to coexist even at room tem-

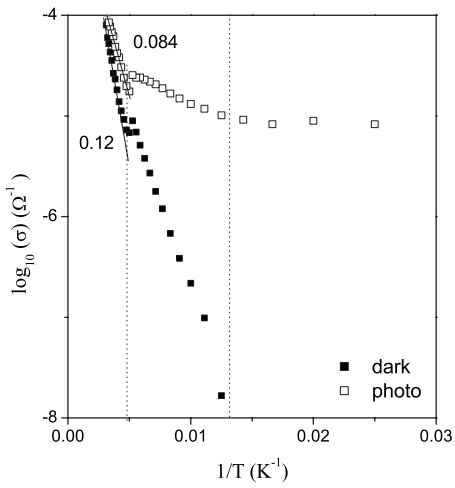

FIG. 1. Dark and photoconductance plotted as $\ln(\sigma)$ vs $1/T$. Straight lines are fits to Arrhenius law. A discontinuity at 190 K is to be noticed, in view of a marked discontinuous increase in conductance at the $M_2 \rightarrow T$ transition temperature in Cr-doped VO_2 single crystals.

perature and the conductance data above 200 K was well fitted by the Arrhenius law, giving an activation energy of ~0.12 eV for dark conductance and ~0.084 eV for photoconductance. The activation energy is much smaller than those of pristine and Cr-doped VO_2 single crystals,[1,12] but is very close to that of Nb-doped VO_2 single crystals,[1,14] for which their hopping mobility is responsible for the activation energy.[1]

The small discontinuity in the conductance is to be noted in Fig. 1 at 190 K in the nanorods, in view of a marked discontinuous increase in conductance at the $M_2 \rightarrow T$ transition temperature in Cr-doped VO_2 single crystals.[1] As in the latter case,[1–4] successive $M_2 \rightarrow T \rightarrow M_1$ structural phase transitions with decreasing temperature may be expected in VO_2 nanorods at 190 and 80 K where magnetic and electrical anomalies take place, in view of a mixed phase of R and M_2 being observed at room temperature. Thus, the discontinuity in the conductance at 190 K may readily be ascribed to the $M_2 \rightarrow T$ transition in the nanorods system, the $M_2 \rightarrow T$ and $T \rightarrow M_1$ transitions being known to be of first and second orders, respectively.[1]

The magnetic susceptibility was reported to decrease with decreasing temperature at the $M_2 \rightarrow T$ transition in Cr-doped VO_2 single crystals,[2] contrasting to the continual increase in the magnetic susceptibility in the nanorods.[15] Half of vanadium ions pair in the M_2 phase and further pairing proceeds in the T phase to a complete pairing of all the vanadium ions in the M_1 phase.[1–3] The decrease in magnetic susceptibility at the $M_2 \rightarrow T$ transition is due to the spin dimerization. In the Nb-doped VO_2 single crystals, however, it was suggested that the itinerant (doped) electron wandering back and forth inside a V^{4+} pair may give rise to a $S=3/2$ state, polarizing both spins parallel to its own spin.[1] An increase in the spin-polarized pairs in the T phase by a gradual carrier localization on the V^{4+} pairs may account for the increase in magnetic susceptibility with decreasing temperature between 90 and 190 K that takes place in the nanorods.[15]

The magnetic susceptibility of the nanorods obeyed the Curie–Weiss law above 190 K and below 90 K with quite distinct Curie–Weiss temperatures of −353 and −13.5 K, respectively.[15] The Curie constant obtained below 90 K is about a half to that obtained above 190 K, being previously unnoticed.[15] While unpaired $S=1/2$ V^{4+} ions are responsible for the Curie–Weiss behavior above 190 K, spin-polarized $S=3/2$ pairs may be responsible for the Curie–Weiss behavior below 90 K. From the Curie constants, we can estimate that ~20% of the unpaired V^{4+} ions become spin-polarized pairs below 90 K, with the rest of them becoming antiferromagnetic spin dimers, amounting to ~0.05 doped-electrons per vanadium atom to be consistent with the small Curie–Weiss temperature. In accordance, the changes in the magnetic susceptibility and the electrical conductance of the nanorods at 190 and 80 K are believed to mark, respectively, the $M_2 \rightarrow T$ and the $T \rightarrow M_1$ transitions having to do with the spin-polarized pairs. While the structural properties of VO_2 nanorods appear to be similar to those of Cr-doped VO_2 single crystals, the spin states of the nanorods appear to be similar to those of Nb-doped VO_2 single crystals.

The photoconductance of the nanorods below 80 K was nearly independent of temperature, while the photoconductivity of VO_2 single crystals showed a strong dependence on temperature at low temperatures and was explained to be related to the depth below the mobility edge to which the localized levels are occupied.[13] In this context, the temperature-independent photoconductance indicates that all the states below the mobility edge in the conduction band are occupied below 80 K. The itinerant (doped) electrons surrounded by the spin cloud with a greatly enhanced effective mass, having to do with the onset of Anderson localization[1] and with the localization of the itinerant carriers on a V^{4+} pair in the localized description, can be considered to occupy the states below the mobility edge in the band picture.

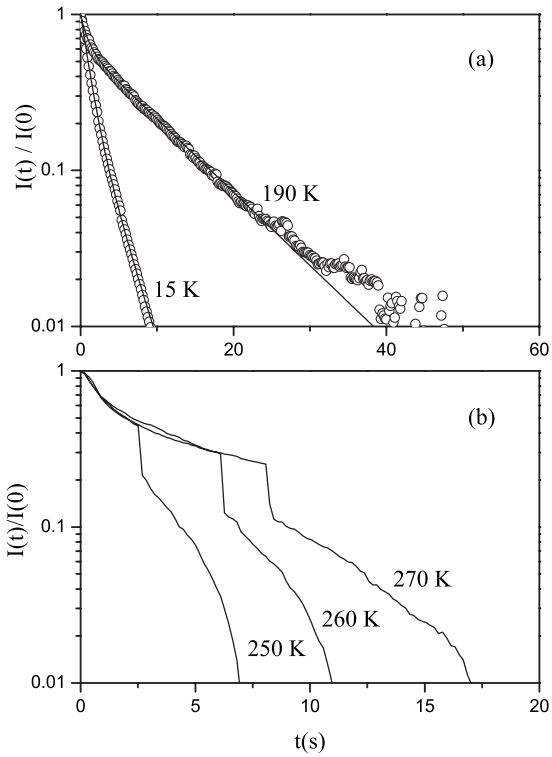

FIG. 2. Photocurrent decay curves at some chosen temperatures. The decay curves below 190 K (a) were fitted by the double-exponential function, and the complicated decay curves above 200 K (b) appear to have to do with the coexisting metallic (R) and insulating (M_2) phases.

Figure 2 shows the photocurrent decay curves at some chosen temperatures. Below 200 K, the decay curves were well fitted by the double-exponential function with short (τ_1) and long (τ_2) time constants [Fig. 2(a)]. The photocurrent decay observed in VO_2 nanorods is distinct from the cases in other vanadium oxide nanostructures such as nanowires and nanotubes, where a single-exponential type of photocurrent decay was observed at least in the low-temperature region.[18,19] Above 200 K, the photocurrent decay curves were too complicated for the decay times to be readily given [Fig. 2(b)], presumably having to do with the coexisting metallic (R) and insulating (M_2) phases. At high temperatures (in the mixed phase) the long-lived photoexcited carriers can encounter the interfaces between the two phases, where a number of the carriers can abruptly relax to their ground states giving rise to the discontinuity in the photocurrent decay curves.

Figure 3 shows the photocurrent decay constants and their fractions. The short decay constant τ_1 being independent of temperature indicates that the short time decay can be ascribed to the large lattice relaxation model where the photoexcited carriers arise from the deep levels within the gap.

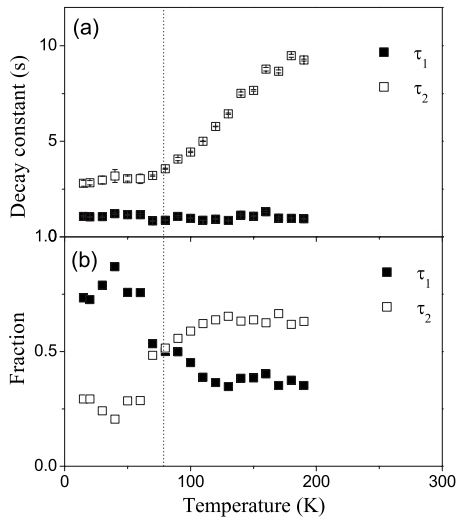

FIG. 3. (a) Photocurrent decay constants and (b) their fractions as a function of temperature. The short decay constant τ_1 being independent of temperature indicates that the short time decay can be ascribed to the large lattice relaxation model, and the long decay constant τ_2 increasing with increasing temperature between 80 and 190 K is compatible with the random local-potential fluctuation model.

The long decay constant τ_2 was independent of temperature below ~80 K, also compatible with the large lattice relaxation model.[19,20] On the other hand, τ_2 increasing with increasing temperature between 80 and 190 K is compatible with the random local-potential fluctuation model, where the photoexcited carriers are stored in the lowest conduction energy levels arising from the local-potential fluctuation.[18,19,21] With increasing temperature, the photoexcited carriers stored in the lowest conduction energy level can hop more easily to the next minimum potential site in the conduction band without recombination to the valance band, and tend to spend more time in there as they experience the minimum potential energies and there are not many holes to recombine with, giving rise to the increase in the relaxation time.[18,21]

The temperature-independent decay constants below 80 K [Fig. 3(a)] indicate that most carriers are localized in deep levels, being consistent with the localization of the itinerant (doped) electrons on the spin-polarized V^{4+} pairs as discussed above. τ_2 decreasing with decreasing temperature between 80 and 190 K also supports a gradual localization of carriers. On the other hand, τ_1 being independent of temperature at all temperatures may indicate localization centers other than the spin-polarized pairs, accounting for ~80% of all the photocarriers below ~80 K. In a previous work on Nb-doped VO_2 single crystals,[1] it was suggested that at low temperatures the itinerant electrons may be localized on one of the V^{4+} ions of a pair, rather than forming a spin-polarized pair, creating a $(S=1)$ V^{3+} ion and leaving the other V^{4+} with an unpaired $(S=1/2)$ electron. Thus, the V^{3+} ions with an electron binding stronger than in the spin-polarized state may readily account for the temperature-independent behavior of τ_1, as well as its fraction becoming dominant below 80 K [Fig. 3(b)].

In summary, we have employed electrical conductivity and photocurrent decay measurements in order to investigate the nature of the physical properties of VO_2 nanorods obtained by hydrothermal treatment of V_2O_5 xerogels. While the electrical (photo)conductivity as well as the magnetic susceptibility of the nanorods may be explained in terms of the $M_2 \rightarrow T \rightarrow M_1$ phase transitions observed in (bulk) Cr-doped VO_2, the charge and spin dynamics appear to be closer to the case of (bulk) Nb-doped VO_2. The itinerant (doped) electron in the VO_2 nanorods may be localized on a V^{4+} pair with decreasing temperature, forming a spin-polarized $(S=3/2)$ pair or creating a $(S=1)$ V^{3+} ion out of a V^{4+} ion pair, apparently accounting for the magnetic properties and the photocurrent decay.

This work was supported by the Korean Ministry of Education, Science and Technology (NRL Program R0A-2008-000-20066-0, User Program of Proton Engineering Frontier Project, Grant No. KRF-2006-005-J03601) and by the Seoul Research and Business Development Program (Grant No. 10583). The measurements at the Korean Basic Science Institute (KBSI) are acknowledged.

[1] A. Zylbersztejn and N. F. Mott, Phys. Rev. B **11**, 4383 (1975).
[2] J. P. Pouget, H. Launois, T. M. Rice, P. Dernier, A. Gossard, G. Villeneuve, and P. Hagenmuller, Phys. Rev. B **10**, 1801 (1974).
[3] M. Marezio, D. B. McWhan, J. P. Remeika, and P. D. Dernier, Phys. Rev. B **5**, 2541 (1972).
[4] J. Magarino, J. Tuchendler, and J. P. D'Haenens, Phys. Rev. B **14**, 865 (1976).
[5] P. Lederer, H. Launois, J. P. Pouget, A. Casalot, and G. Villeneuve, J. Phys. Chem. Solids **33**, 1969 (1972).
[6] J. P. Pouget, P. Lederer, D. S. Schreiber, H. Launois, D. Wohlleben, A. Casalot, and G. Villeneuve, J. Phys. Chem. Solids **33**, 1961 (1972).
[7] J. P. Pouget, H. Launois, J. P. D'Haeneus, P. Merenda, and T. M. Rice, Phys. Rev. Lett. **35**, 873 (1975).
[8] S. Biermann, A. Poteryaev, A. I. Lichtenstein, and A. Georges, Phys. Rev. Lett. **94**, 026404 (2005).
[9] T. M. Rice, H. Launois, and J. P. Pouget, Phys. Rev. Lett. **73**, 3042 (1994).
[10] T. Kawakubo, J. Phys. Soc. Jpn. **20**, 516 (1965).
[11] W. Chen, J. Peng, L. Mai, H. Yu, and Y. Qi, Chem. Lett. **33**, 1366 (2004).
[12] W. H. Rosevear and W. Paul, Phys. Rev. B **7**, 2109 (1973).
[13] G. von Schulthess and P. Wachter, Solid State Commun. **15**, 1645 (1974).
[14] G. Villeneuve, A. Bordet, A. Casalot, J. P. Pouget, H. Launois, and P. Lederer, J. Phys. Chem. Solids **33**, 1953 (1972).
[15] J. Park, I. H. Oh, E. Lee, K. W. Lee, C. E. Lee, K. Song, and Y. Kim, Appl. Phys. Lett. **91**, 153112 (2007).
[16] R. Lopez, T. E. Haynes, L. A. Boatner, L. C. Feldman, and R. F. Haglund, Jr., Phys. Rev. B **65**, 224113 (2002).
[17] R. Lopez, R. F. Haglund, Jr., L. C. Feldman, L. A. Boatner, and T. E. Haynes, Appl. Phys. Lett. **85**, 5191 (2004).
[18] J. Park, E. Lee, K. W. Lee, and C. E. Lee, Appl. Phys. Lett. **89**, 183114 (2006).
[19] H. Kweon, K. W. Lee, and C. E. Lee, Appl. Phys. Lett. **93**, 043105 (2008).
[20] D. V. Lang and R. A. Logan, Phys. Rev. Lett. **39**, 635 (1977).
[21] H. X. Jiang and J. Y. Lin, Phys. Rev. B **40**, 10025 (1989).